

Non-peptidic Inhibitors of Human Leukocyte Elastase. 1. The Design and Synthesis of Pyridone-Containing Inhibitors

Peter Warner,^{*,†,§} Rosalyn C. Green,[†] Bruce Gomes,[‡] and Anne M. Strimpler[‡]

Departments of Medicinal Chemistry and Pharmacology, Zeneca Pharmaceuticals Group, A Business Unit of ZENECA Inc., 1800 Concord Pike, Wilmington, Delaware 19897

Received April 29, 1994[®]

Human leukocyte elastase (HLE) is a serine protease produced by neutrophils that has been implicated in diseases such as emphysema and cystic fibrosis. An HLE inhibitor may have therapeutic value in these diseases. An active site model of HLE bound to a tripeptidic trifluoromethyl ketone (TFMK) inhibitor, **2**, was created from X-ray structures of HLE and porcine pancreatic elastase. Analysis of the model indicated a preferred binding conformation for the tripeptide and potentially important interactions between it and the enzyme. This information was used to aid in the design of a series of novel, pyridone-containing, non-peptidic HLE inhibitors such as 2-[3-[[benzyloxy]carbonyl]amino]-2-oxo-1,2-dihydro-1-pyridyl]-N-(3,3,3-trifluoro-1-isopropyl-2-oxopropyl)acetamide (**5b**) ($K_i = 280 \pm 78$ nM). Inspection of the active site model suggested that a benzyl substituent at the 5-position of the pyridone ring might improve potency by forming a lipophilic interaction with the enzyme S2 pocket. Synthesis and biological evaluation of a series of 5-benzylpyridone TFMKs provided evidence for this proposition. Further analysis of the model indicated that substitution on the 3-amino group of the pyridone ring with a hydrogen bond acceptor could potentially lead to interactions with the NH atoms of glycine-218 and/or -219. The oxalate derivative 2-[5-benzyl-3-(carboxycarbonyl)-2-oxo-1,2-dihydro-1-pyridyl]-N-(3,3,3-trifluoro-1-isopropyl-2-oxopropyl)acetamide (**5v**) was synthesized and found to have a K_i of 48 ± 9 nM. Unfortunately, none of the compounds tested was active in an *in vivo* model of HLE-induced lung injury when dosed orally.

Introduction

Human leukocyte elastase (HLE) (EC 3.4.21.37) is a member of the serine protease family of enzymes produced by polymorphonuclear leukocytes (PMNs) and has a molecular weight of about 30 kDa. It is released from PMNs in response to inflammatory stimuli¹ and has been implicated in the development of various diseases such as emphysema,²⁻⁴ ARDS,^{5,6} cystic fibrosis,⁷⁻⁹ and rheumatoid arthritis.¹⁰ Under normal conditions, the body protects itself from the potentially damaging effects of extracellular HLE with the endogenous inhibitor α_1 -proteinase (α_1 -PI). However if the balance between protease and anti-protease is upset due to a decrease in levels of α_1 -PI, the excess HLE activity may lead to tissue damage and the development of a disease such as emphysema.¹¹ This imbalance can occur in cigarette smokers because of the oxidative inactivation of α_1 -PI by the smoke.^{12,13} Alternatively, the quantity of α_1 -PI synthesized may be inadequate due to a genetic defect.¹¹ In both cases, the excess HLE hydrolyzes elastin, the structural protein which gives the lung its elasticity, and contributes to development of the disease.

It has been hypothesized that an appropriate, small molecular weight inhibitor of HLE will restore the imbalance between HLE and α_1 -PI in diseases such as emphysema and be useful therapeutically in the treatment of such diseases.¹⁴ A variety of structural classes of HLE inhibitors have been reported, including the

peptidyl trifluoromethyl ketones¹⁵⁻¹⁸ (TFMKs), the α -ketobenzoxazoles,¹⁹ the β -lactams,²⁰ and others.¹⁴ TFMK compounds such as ICI 200,880 (**1**) are highly potent HLE inhibitors *in vitro* and possess activity in *in vivo* models of acute lung injury.^{21,22} ICI 200,880 (**1**) is currently being evaluated in the clinic for efficacy in a range of HLE-mediated disorders.

TFMK inhibitors like **1** are thought to act by trapping the active site serine-195 hydroxyl group. According to this hypothesis, the highly electrophilic character of the TFMK facilitates the enzyme-catalyzed addition of the serine-195 hydroxyl to the ketone of the inhibitor. The resulting hemiketal is an analogue of the tetrahedral intermediate formed in the normal hydrolysis reaction of the peptide bond catalyzed by HLE, but this hemiketal is unable to proceed to products. This proposed mechanism of reversible inhibition has been proved for the related porcine pancreatic elastase (PPE) by X-ray analysis of the complex formed between PPE and a TFMK inhibitor.²³ The high-resolution X-ray structure contains a covalent bond (1.5 Å) between the serine-195 oxygen and the TFMK carbonyl carbon center.

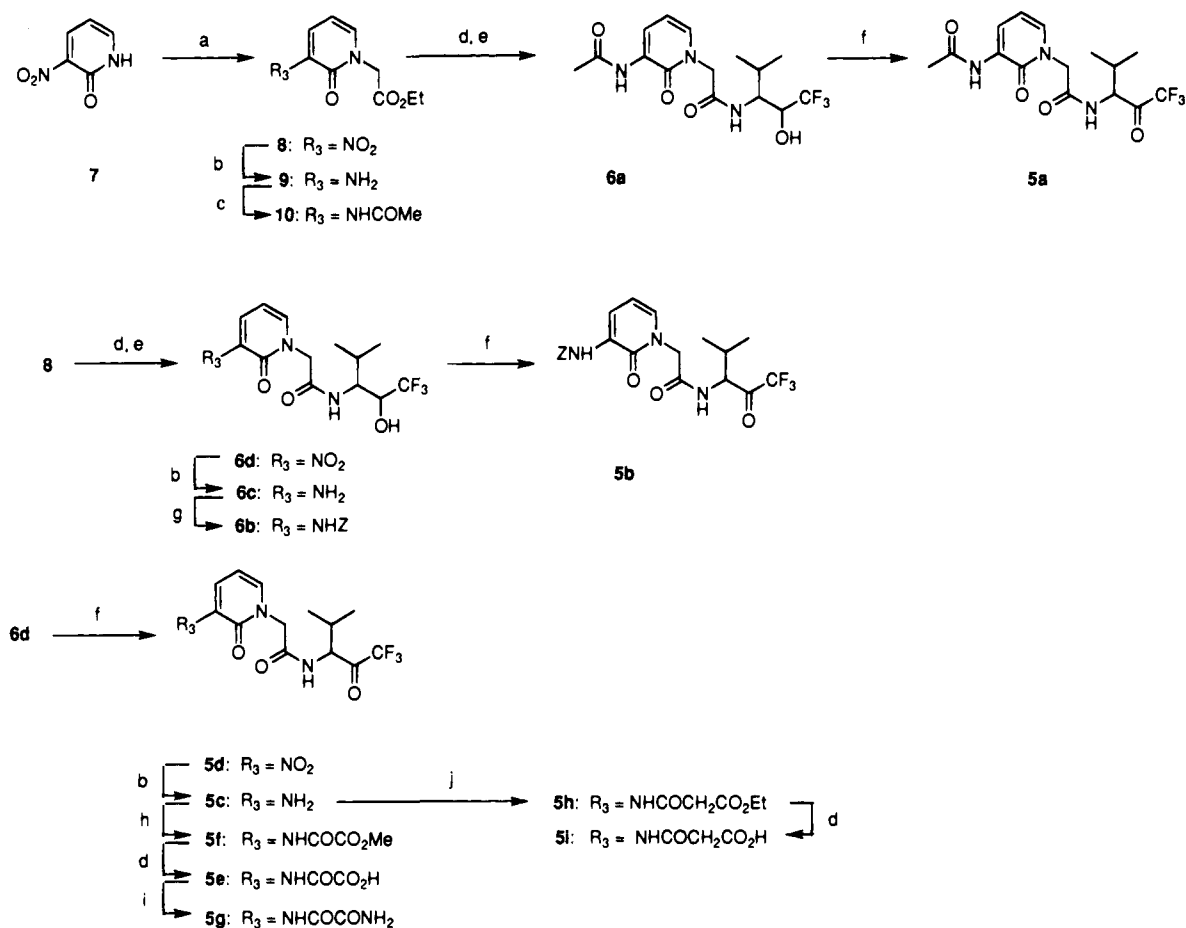
A potential drawback of peptidic HLE inhibitors as drugs is the possible instability of the peptidic backbone to metabolism. ICI 200,880 (**1**) is potent in animal models of lung damage when dosed intratracheally *via* an aerosol to the lung surface, but its systemic activity in similar models is somewhat less.²¹ Another problem with peptidic TFMKs is the stereochemical complexity of the peptides in conjunction with the ready epimerization of the chiral center adjacent to the TFMK, which leads to formation of diastereoisomeric mixtures. For these reasons, it was considered desirable to design non-peptidic and stereochemically less complex TFMK in-

[†] Department of Medicinal Chemistry.

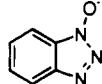
[‡] Department of Pharmacology.

[§] Present address: ZENECA Pharmaceuticals, Mereside, Alderley Park, Macclesfield SK10 4TG, U.K.

[®] Abstract published in *Advance ACS Abstracts*, August 15, 1994.

Scheme 1^a

^a Reagents: (a) (1) NaH, DMF, (2) ethyl iodoacetate; (b) H₂, 10% Pd-C, EtOH; (c) acetic anhydride, Na₂CO₃; (d) 1M aqueous NaOH, MeOH; (e) 3-amino-4-methyl-1,1,1-trifluoro-2-pentanol HCl (21), EDC, DMAP, DMF; (f) EDC, dichloroacetic acid, DMSO, toluene; (g) benzyl chloroformate, sodium carbonate, THF; (h) ClCOCH₂CO₂Me, triethylamine, CH₂Cl₂, 0 °C; (i) ClCOCH₂CO₂H, triethylamine, CH₂Cl₂, 0 °C; (j) ClCOCH₂CO₂Et, triethylamine, CH₂Cl₂, 0 °C.



inhibitors. Our initial approaches to this problem are the subject of this paper.

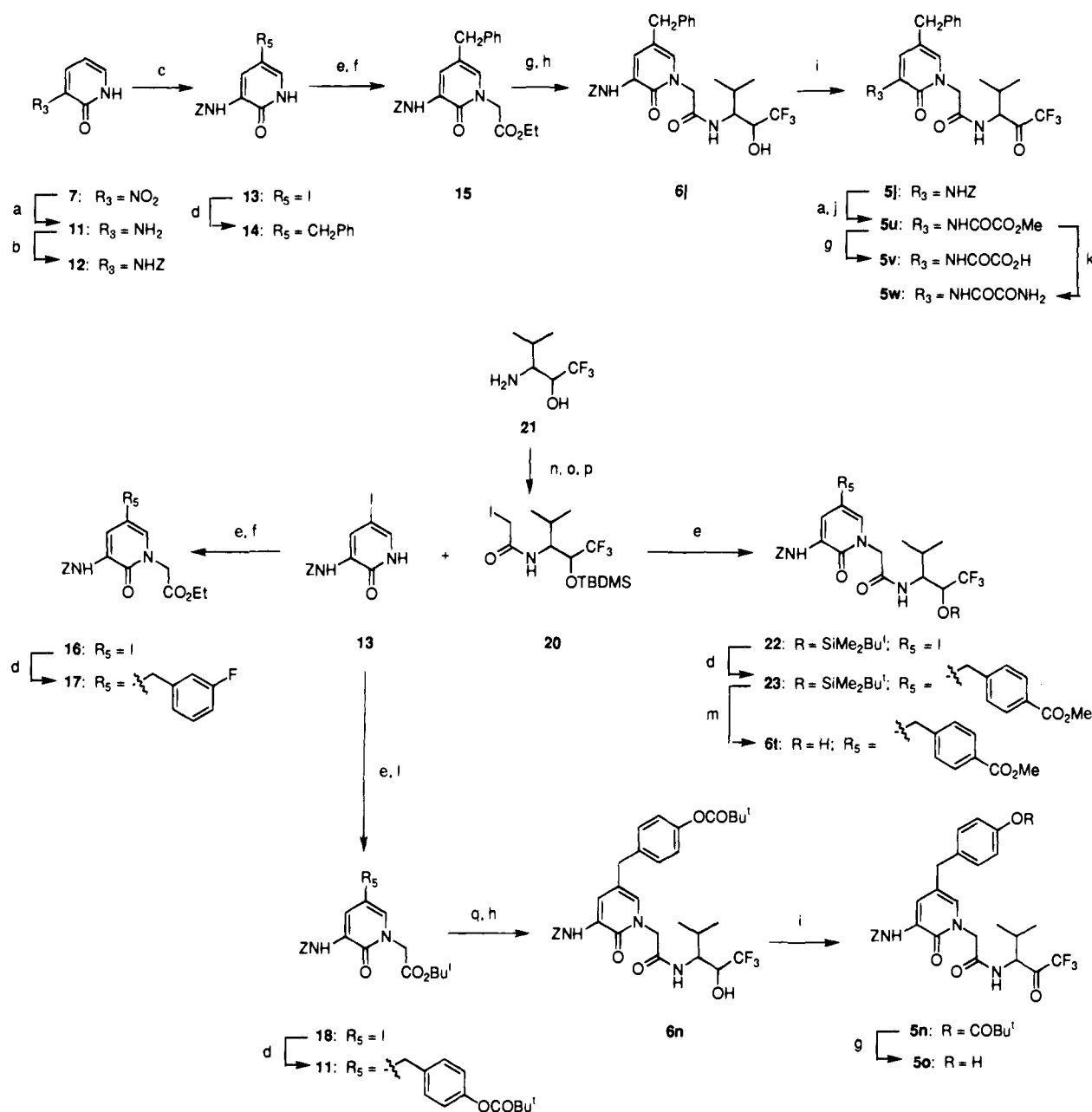
Chemistry

The compounds described in this paper were prepared by the general methods illustrated in Schemes 1 and 2. Representative methodology is detailed in the Experimental Section, and Table 1 provides the sequence of steps used for the synthesis of each compound.

The anion derived from commercially available 3-nitropyrid-2-one (7) was alkylated at the nitrogen by ethyl iodoacetate to give compound 8. The trifluoromethyl alcohols 6a–d were prepared from 8 by either the sequence of hydrogenation, acylation, aqueous hydrolysis, and amide coupling to give 6a or the sequence of hydrolysis and amide coupling to give 6d, hydrogenation to 6c, and acylation to 6b. The trifluoromethyl alcohols 6a,b,d were oxidized directly to the corresponding ketones 5a,b,d by a modification of the Pfizner–Moffatt procedure utilizing 1-[3-(dimethylamino)propyl]-3-ethylcarbodiimide hydrochloride (EDC).^{24,25} TFMK 5d was hydrogenated to the amino TFMK 5c which was elaborated to the oxalate (5e–g) and malonate (5h,i) derivatives using standard methods (Scheme 1).

The 5-benzylpyridone TFMKs were synthesized by analogous routes to those used for the unsubstituted compounds (Scheme 2). The 5-benzyl groups were introduced *via* palladium-catalyzed zinc coupling with the iodo compounds 13, 16, 18, and 22. The optimal catalyst for this reaction was found to be dichloro[1,1'-bis(diphenylphosphino)ferrocene]palladium(II).²⁶ Other more conventional catalysts gave lower yields or no reaction. The precursor iodo compound 13, from which the substituted iodo compounds 16, 18, and 22 were derived, was synthesized from pyridone 12 by selective 5-iodination with *N*-iodosuccinimide.

A particularly convergent method of synthesizing TFMK compounds with a variety of functional groups attached to the phenyl ring of the 5-benzyl substituent was developed. The pyridone compound 13 was alkylated with 20²⁶ to give 22 (Scheme 2). This compound was converted to the 4-(methoxycarbonyl)benzyl derivative 6t by the sequence of palladium-catalyzed coupling with [4-(methoxycarbonyl)benzyl]zinc bromide, desilylation by fluoride anion, and oxidation. An alternative method employed in the synthesis of 5n involved alkylation of 13 with *tert*-butyl bromoacetate, palladium-catalyzed coupling with [4-(pivaloyloxy)benzyl]-

Scheme 2^a

^a Reagents: (a) H₂, 10% Pd-C, EtOH; (b) benzyl chloroformate, sodium carbonate, THF; (c) *N*-iodosuccinimide, CH₂Cl₂; (d) Zn, ArCH₂Br, THF, dichloro[1,1'-bis(diphenylphosphino)ferrocene]Pd(II); (e) NaH, DMF; (f) ethyl iodacetate, DMF; (g) 1 M aqueous NaOH, MeOH; (h) 21, EDC, DMAP, DMF; (i) EDC, dichloroacetic acid, DMSO, toluene; (j) ClCOCO₂Me, triethylamine, CH₂CH₂, 0 °C; (k) NH₄OH, MeOH; (l) *tert*-butyl bromoacetate, DMF; (m) tetrabutylammonium fluoride, THF; (n) ClCH₂COCl, 4-methylmorpholine, THF; (o) *tert*-butyldimethylsilyl triflate, 2,6-lutidine, CH₂Cl₂; (p) NaI, acetone; (q) TFA.

zinc bromide, selective hydrolysis of the *tert*-butyl ester of **11** with trifluoroacetic acid, coupling with **21**, and oxidation to give **5n** (Scheme 2).

Biological Evaluation

The compounds listed in Table 1 were tested *in vitro* for their ability to inhibit HLE activity. The inhibition constants (*K_i*), corresponding to the ability of the compounds to inhibit hydrolysis of the synthetic substrate MeO-Suc-Ala-Ala-Pro-Val-pNA, were determined as previously described.²¹

Molecular Modeling

It was our aim to use protein structural information in conjunction with molecular modeling techniques to

facilitate the design of novel HLE inhibitors. X-ray crystal structures of elastases, either native or bound to inhibitors, were available.²⁸ However, there were no reports of a crystallographically determined structure of HLE bound to a TFMK inhibitor. It was necessary, therefore, to create a model of the active site of HLE bound to a TFMK inhibitor. As a starting point, the crystal structures of HLE bound to the turkey ovomucoid inhibitor third domain (TOMI)²⁹ and PPE bound to a tripeptidic inhibitor, **2**²³ (Figure 1), were considered. Initially it was necessary to model the peptidic inhibitor **2** into the active site of HLE as described below. Such an approximation is feasible because the active site homology between HLE and PPE is high.²⁸

In order to facilitate the modeling work, a simplified

Table 1. Preparation and *in Vitro* Activities of Pyridone TFMKs^a

compd	R ³	R ⁵	method ^b	mp, °C	formula ^c	K _i , nM
5a	NHCOMe	H	D,A,B,F,G	76–80	C ₁₅ H ₁₈ F ₃ N ₃ O ₄ ·H ₂ O	2800 ± 400
5b	NHZ ^d	H	D,F,A,B,G	58–61	C ₂₁ H ₂₂ F ₃ N ₃ O ₅ ·0.33H ₂ O	280 ± 78
5c	NH ₂	H	D,F,G,A	135 dec	C ₁₃ H ₁₆ F ₃ N ₃ O ₃ ·0.5H ₂ O ^e	2700 ± 500
5d	NO ₂	H	D,F,G	60–65	C ₁₃ H ₁₄ F ₃ N ₃ O ₅ ·H ₂ O	15000 ± 5000
5e	NHCOCO ₂ H	H	D,F,G,A,B,F ^f	168–170	C ₁₅ H ₁₆ F ₃ N ₃ O ₆ ·0.33H ₂ O	350 ± 70
5f	NHCOCO ₂ Me	H	D,F,G,A,B	74–79	C ₁₆ H ₁₈ F ₃ N ₃ O ₆ ·0.75H ₂ O	500 ± 150
5g	NHCOCONH ₂	H	D,F,G,A,B,F, ^f I	258–260	C ₁₅ H ₁₇ F ₃ N ₄ O ₅ ·0.5H ₂ O	320 ± 20
5h	NHCOCH ₂ CO ₂ Et	H	D,F,G,A,B	126–128	C ₁₈ H ₂₂ F ₃ N ₃ O ₆ ·0.25H ₂ O	3400 ± 800
5i	NHCOCH ₂ CO ₂ H	H	D,F,G,A,B,F ^f	84–102	C ₁₆ H ₁₈ F ₃ N ₃ O ₆ ·H ₂ O	2600 ± 200
5j	NHZ	PhCH ₂	A,B,C,E,D,F,G	58–64	C ₂₈ H ₂₈ F ₃ N ₃ O ₅ ·0.75H ₂ O	40 ± 9
5k	NHZ	3-F-C ₆ H ₄ CH ₂	A,B,C,D,E,F,G	64–70	C ₂₈ H ₂₇ F ₄ N ₃ O ₅ ·0.25H ₂ O	87 ± 18
5l	NHZ	4-F-C ₆ H ₄ CH ₂	A,B,C,D,E,F,G	66–72	C ₂₈ H ₂₇ F ₄ N ₃ O ₅ ·0.75H ₂ O	71 ± 15
5m	NHZ	4-CF ₃ -C ₆ H ₄ CH ₂	A,B,C,D,E,F,G	61–65	C ₂₉ H ₂₇ F ₆ N ₃ O ₅ ·H ₂ O	47 ± 13
5n	NHZ	4-Bu ^t OCO-C ₆ H ₄ CH ₂	A,B,C,D,E,L,G	70–77	C ₃₃ H ₃₆ F ₃ N ₃ O ₇ ·0.5H ₂ O	32 ± 18
5o	NHZ	4-HO-C ₆ H ₄ CH ₂	A,B,C,D,E,L,G,F ^f	65–70	C ₂₈ H ₂₈ F ₃ N ₃ O ₆ ·0.75H ₂ O	34 ± 3
5p	NHZ	3-Bu ^t OCO-C ₆ H ₄ CH ₂	A,B,C,D,E,L,G	63–71	C ₃₃ H ₃₆ F ₃ N ₃ O ₇ ·0.5H ₂ O	12 ± 5
5q	NHZ	3-HO-C ₆ H ₄ CH ₂	A,B,C,D,E,L,G,F ^f	63–73	C ₂₈ H ₂₈ F ₃ N ₃ O ₆ ·0.75H ₂ O	89 ± 17
5r	NHZ	3-MeOCO-C ₆ H ₄ CH ₂	A,B,C,D,E,L,G,F,B	59–80	C ₃₀ H ₃₀ F ₃ N ₃ O ₇ ·0.5H ₂ O	42 ± 17
5s	NHZ	3-CF ₃ CONH-C ₆ H ₄ CH ₂	A,B,C,D,E,L,G	159–161	C ₃₀ H ₂₈ F ₆ N ₄ O ₆ ·0.5H ₂ O	36 ± 8
5t	NHZ	4-CH ₃ O ₂ C-C ₆ H ₄ CH ₂	A,B,C,D,E,K,G	68–75	C ₃₀ H ₃₀ F ₃ N ₃ O ₇ ·0.75H ₂ O	88 ± 26
5u	NHCOCO ₂ Me	PhCH ₂	A,B,C,E,D,F,G,A,B	151–157	C ₂₃ H ₂₄ F ₃ N ₃ O ₆	70 ± 22
5v	NHCOCO ₂ H	PhCH ₂	A,B,C,E,D,F,G,A,B,F ^f	82–93	C ₂₂ H ₂₂ F ₃ N ₃ O ₆	48 ± 9
5w	NHCOCONH ₂	PhCH ₂	A,B,C,E,D,F,G,A,B,I	147–156	C ₂₂ H ₂₃ F ₃ N ₄ O ₅ ·0.5H ₂ O	51 ± 12

^a See Schemes 1 and 2 for positions of substituents R³ and R⁵. ^b See Experimental Section for lettered methods. ^c Anal. C, H, N except where stated otherwise. ^d Z is (benzyloxy)carbonyl. ^e N: calcd, 12.8; found, 11.81. ^f First part only of method F used.

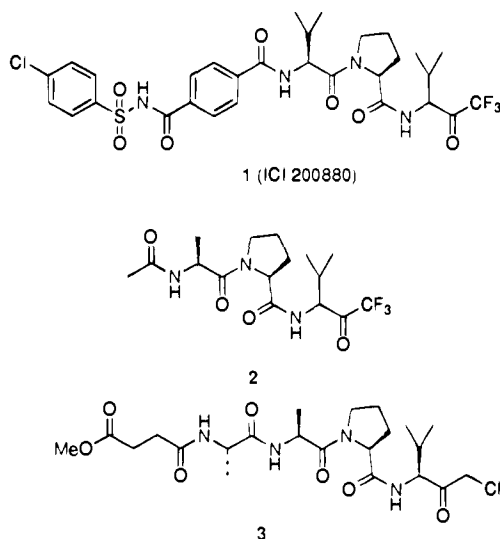


Figure 1. Inhibitors of HLE and PPE.

active site of HLE bound to TOMI was created which included only those parts of HLE believed to form the active site of the enzyme.³⁰ The active site of HLE and the PPE structure were overlaid using ENIGMA.³¹ The serine-195 oxygen of PPE was disconnected from the tripeptide **2**, and the corresponding oxygen of HLE was connected to the inhibitor. The PPE structure was deleted, leaving the TFMK inhibitor **2** modeled in the active site of HLE. The oxyanion was represented by a fluorine atom. Using the molecular mechanics program AESOP,³² the TFMK inhibitor was energy optimized while covalently linked to the active site, which was held rigid during the energy minimization process. The resulting geometry of the tripeptide was very similar to that observed when bound to PPE. To try and improve the quality of the active site model to take into account changes in conformation that might be expected to occur when changing from the noncovalently attached TOMI to the TFMK inhibitor, further energy minimizations were performed allowing parts of the active site, as well as the inhibitor, to relax.³³ The more sophisticated energy minimizations did not change significantly

the conformation of the inhibitor or active site but did lead to an overall lowering of steric energy for the active site model.

A number of simplifications and assumptions were made in the building of the HLE active site model. The model assumes that the conformation and the binding mode of the TFMK tripeptide **2** in HLE are analogous to those observed in PPE. The validity of these assumptions is supported by the similarity between the predicted conformation and the binding modes adopted by the P1–P4 region of TOMI bound to HLE and the P1–P4 region of the chloromethyl ketone inhibitor **3** bound to HLE.³⁴ It is also conceivable that the conformation of the HLE enzyme bound to the TFMK **2** changes from that of the HLE–TOMI complex. However, both the geometries of HLE bound to TOMI and the chloromethyl ketone inhibitor **3** and the geometries of the HLE and PPE active sites are very similar. The active site model was analyzed for the key interactions between the inhibitor and the enzyme that lead to good binding and inhibition of HLE by the TFMK. These key interactions are illustrated schematically in Figure 2a.

The next step was to use the active site model to generate ideas for the design of novel non-peptidic TFMK inhibitors of HLE. At the outset, it was decided to retain the TFMK as an electrophilic trap for the enzyme. Examination of the interaction of the P1 isopropyl group in the S1 pocket indicated that replacing this functionality in a manner consistent with retaining good binding would be very difficult. In contrast, the P2 proline residue makes relatively weak interactions with the enzyme, so attention was focused on this part of the tripeptide.

It has previously been reported that the P2 proline can be replaced successfully with *N*-alkylglycine residues.^{18,35,36} This interesting finding and the lack of specific interactions predicted by the model between the P3 methyl group (R₁ in Figure 2a) and the enzyme suggested that cyclizing a substituent from the P2 nitrogen to the α -carbon of the P3 residue might be feasible.³⁷ We discovered by examination of our HLE

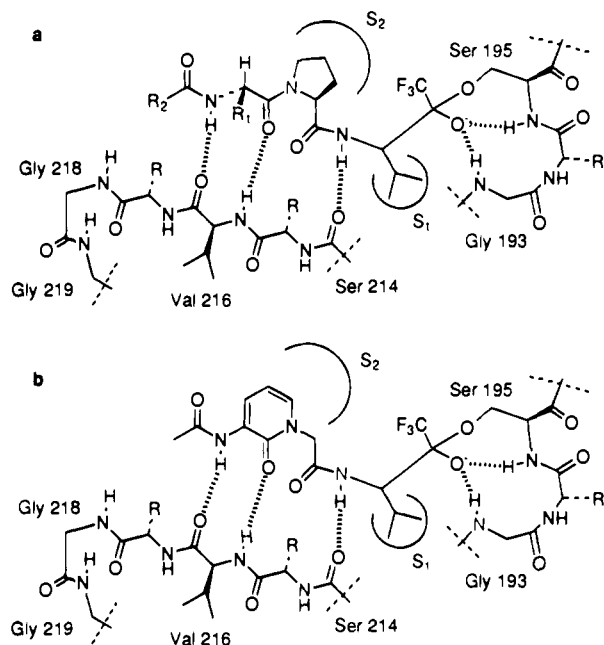


Figure 2. Schematic representation of the key interactions within the active site model of HLE with a peptide inhibitor (a) and a pyridone inhibitor (b).

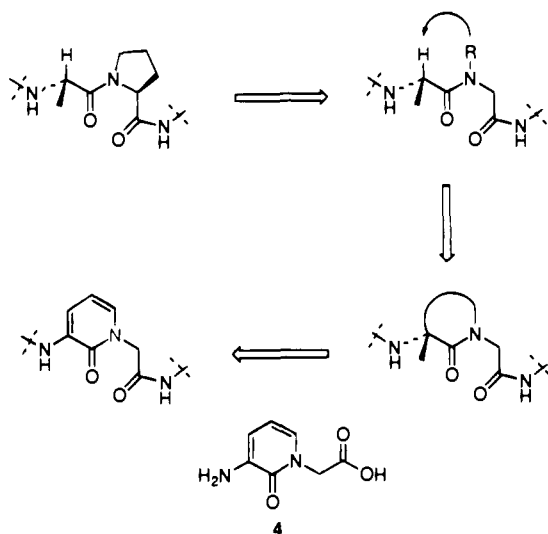


Figure 3. Design of the pyridone dipeptide mimetic.

active site model that the two key hydrogen-bonding interactions between valine-216 and the peptide inhibitor P3 residue (see Figure 2a) might be maintained even if the P3 α -carbon was transformed into an sp^2 hybridized center. This observation provided the possibility of converting the peptidic inhibitor into a non-peptidic, stereochemically less complex heterocyclic system possessing the potential to bind into the active site of HLE. A variety of species containing links between the P2 nitrogen and the α -carbon of the P3 residue were considered, and a pyridone system was selected (Figure 3).

The structure of **2** was modified by replacing the P2 proline and P3 alanine residues with the proposed dipeptide isostere 2-(3-amino-2-oxo-1,2-dihydro-1-pyridyl)acetic acid (**4**). Using ENIGMA, the modified structure **5a** was modeled into the enzyme active site model. It was assumed that the compound would bind in the P1 and oxyanion region of the active site analogously to the peptide TFMK **2**. The molecule was

energy minimized in the active site model. The key interactions predicted for the molecule were similar to those available to the peptide except that there was very little hydrophobic interaction between the compound and the S2 pocket. As anticipated, the disposition of the pyridone NH bond with respect to the valine-216 carbonyl group was quite different compared to that found for the peptide, but the geometry required for a good hydrogen-bonding interaction did seem to be achievable (Figure 2b).

The next step in the modeling process was to assess whether the conformation of **5a** required to bind to the active site as proposed above is readily accessible to the free compound. The key region of conformational flexibility focused on was the N-linked side chain. A search of conformational space was made using the model compound 2-(2-oxo-1,2-dihydro-1-pyridyl)acetamide by systematically varying the torsion angles. Of the several low-energy conformations which were identified, one corresponded to the conformation proposed above for efficient binding to the active site. Therefore, on the basis of this modeling work, compound **5a** became the initial target for synthesis.

Results and Discussion

Compound **5a**, in which the P2 proline and P3 alanine functionality of the peptidic inhibitor **2** are replaced with the putative non-peptidic dipeptide mimic **4** (Figure 3), was synthesized. The compound (**5a**) was found to be an inhibitor of HLE with a K_i of 2800 ± 400 nM. This key result demonstrated that the pyridone system is a viable isosteric replacement for the P3–P2 residues found in peptidic TFMK inhibitors of HLE.

There is precedent from the peptide series of inhibitors that HLE will accept a wide variety of substituents in the S4 subsite.³⁸ These substituents may be acidic, basic, or neutral, and lipophilicity is generally advantageous. The terminal methyl group of **5a** is unlikely to form a good interaction with the enzyme; however, a benzyloxy substituent appears to fit well into the active site with the potential to make lipophilic interactions with the S4 subsite. To evaluate this prediction, compound **5b** was synthesized and found to be 10 times more potent ($K_i = 280 \pm 78$ nM) than compound **5a**.

An examination of how the benzyloxy substituent might bind into the S4 region of HLE led to the observation that the ether oxygen approached quite closely to two amide hydrogen atoms in the enzyme active site. The backbone NH bonds of glycine-218 and -219 (Figure 2b) point toward the 3-substituent of the pyridone ring and are disposed analogously to the NH bonds that form part of the characteristic "oxyanion-binding" region between the S1 and S'1 pockets of serine proteases. It appeared that careful selection of an appropriate pyridone 3-substituent might permit the formation of another hydrogen-bonding interaction between the inhibitor and the enzyme. A properly oriented carbonyl group would have the potential to bind well with at least one of the two free NH groups. It was proposed that this interaction could be achieved by appending an oxalate group to the 3-amino group of the pyridone ring. Thus, the oxalate compound **5e** was synthesized and found to have a K_i of 350 ± 70 nM. This level of potency is comparable with that of the much more lipophilic (benzyloxy)carbonyl compound **5b**. The

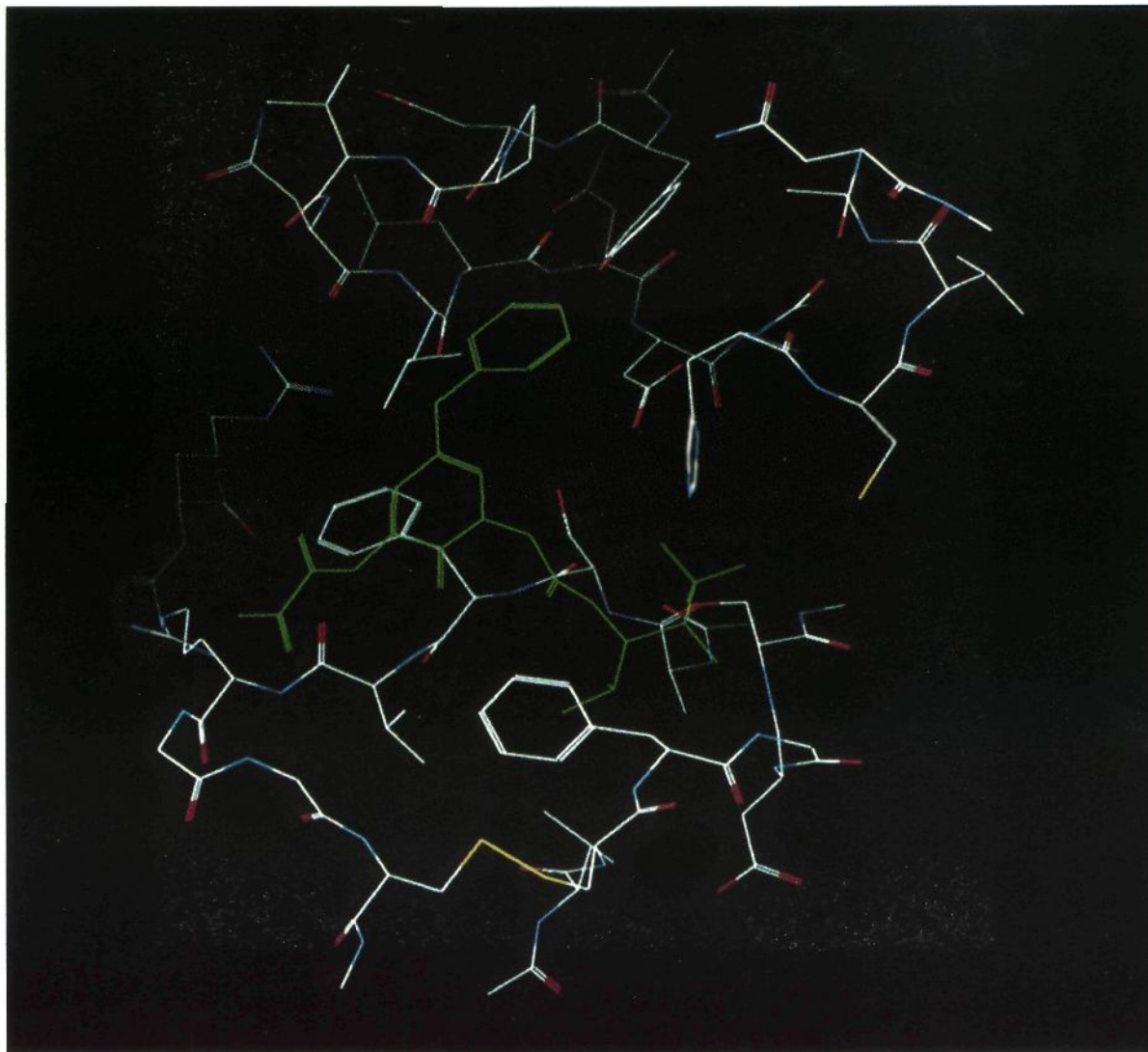


Figure 4. Compound **5v** (colored green) modeled into the HLE active site.

corresponding malonyl derivative **5i** is significantly less potent (K_i of 2600 ± 200 nM), consistent with the prediction that it should be unable to interact effectively with either of the NH groups. The methyl ester **5f** and the primary amide **5g** were found to have similar potencies to the parent oxalate **5e**. These data indicate that the compounds may interact as predicted from the active site model with the NH groups of glycine-218 and/or -219 via the carboxy carbonyl oxygen.

It is apparent from inspection of data produced on HLE inhibitors from the peptidic series that a lipophilic substituent at P2 is important for high potency.¹⁸ This is likely to be due to the effects of the substituents on conformational restriction as well as increased hydrophobic binding. Examination of **5b** in the active site model led to the observation that a benzyl substituent attached to the 5-position of the pyridone ring might bind into the S2 pocket to provide a specific lipophilic interaction. Conformational analysis of the 5-benzylpyridone system identified the two lowest energy conformations available to the molecule. Modeling of compound **5j** in either of the two favorable "5-benzyl" conformations indicated that both could potentially fit into the active site and thereby increase the degree of van der Waals interactions between the putative inhibi-

tor and the enzyme. Therefore, compound **5j** was synthesized and found to be a potent inhibitor of HLE ($K_i = 40 \pm 9$ nM). An enzyme kinetic analysis of compound **5j** showed that it is a reversible and competitive inhibitor. It is very selective for HLE even against closely related enzymes (PPE, $K_i = 140$ μ M; trypsin, no inhibition at 20 μ M; thrombin, $K_i = 140$ μ M). A limited series of compounds was prepared with various substituents incorporated into the 5-benzyl ring. The effect on potency was relatively small. A 3-fold improvement in potency to $K_i = 12 \pm 5$ nM was observed for compound **5p** containing the bulky and lipophilic pivaloyloxy substituent in the *meta* position.

Incorporation of the 5-benzyl substituent into the oxalate compound **5e** and the oxalate methyl ester **5f** to give compounds **5v** ($K_i = 48 \pm 9$ nM) and **5u** ($K_i = 70 \pm 22$ nM) similarly led to improvements in potency compared with the parent compounds. Figures 4 and 5 illustrate oxalate derivative **5v** (colored green) modeled into the active site of HLE. The proposed key interactions of the enzyme with the heterocyclic ring and the oxalate and benzyl side chains are clearly apparent.

Representative compounds (**5g,j,m,v,w**) were evaluated for activity in an acute lung hemorrhagic model.²¹ This assay measures the ability of the inhibitor to

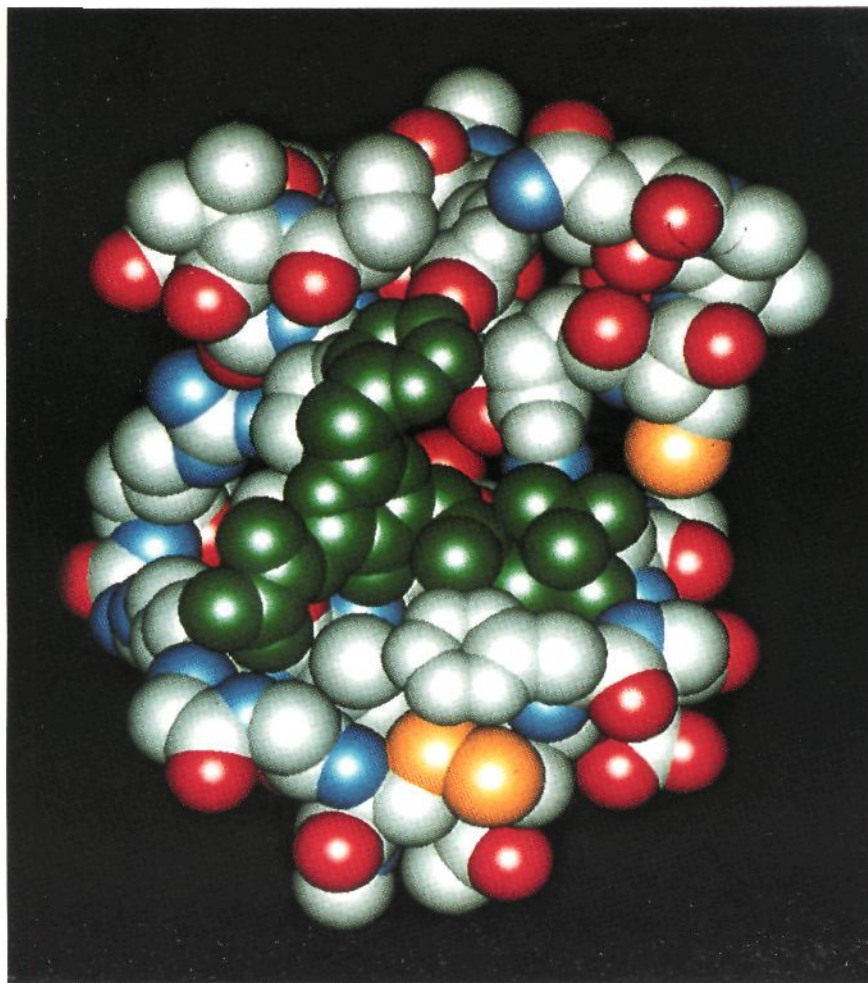


Figure 5. Compound **5v** (colored green) modeled into the HLE active site.

protect the lung from hemorrhage induced by the instillation of HLE into the trachea of anaesthetized hamsters 30 min after oral administration of the inhibitor. The amount of hemorrhage is measured by the spectrophotometric determination of the amount of hemoglobin present in a lung lavage sample. Disappointingly, none of the compounds tested showed statistically significant protection of HLE-induced lung hemorrhage. To determine whether measurable blood levels of inhibitor were obtained after oral dosing, a 75 mg/kg dose of **5v** was given to hamsters followed by determination of plasma levels using a published method.²¹ No **5v** was detected in this experiment, indicating that the lack of oral activity may be due to poor absorption or extensive first-pass metabolism.

In conclusion, we have used X-ray crystallographic information and molecular modeling techniques to design rationally a new series of potent, selective, and non-peptidic HLE inhibitors and a new dipeptide isostere, **4**. The results of our efforts to increase *in vitro* potency and obtain *in vivo* activity in this series have been reported in preliminary form³⁹ and will be reported in full separately.

Experimental Section

General Procedures. Analytical samples were homogeneous by TLC and afforded spectroscopic results consistent with the assigned structures. Proton NMR spectra were obtained using either a Bruker WM-250 or AM-300 spectrom-

eter. Chemical shifts are reported in parts per million relative to Me₄Si as internal standard. Mass spectra (MS) were recorded on a Kratos MS-80 instrument operating in the chemical ionization (CI) mode. Elemental analyses for carbon, hydrogen, and nitrogen were determined by the ICI Americas Analytical Department on a Perkin-Elmer 241 elemental analyzer and are within $\pm 0.4\%$ of theory for the formulae given. Analytical thin-layer chromatography (TLC) was performed on precoated silica gel plates (60F-254, 0.2 mm thick; E. Merck). Visualization of the plates was accomplished by using UV light or phosphomolybdic acid/ethanol-charring procedures. Chromatography refers to flash chromatography conducted on Kieselgel 60 230–400 mesh (E. Merck, Darmstadt) using the indicated solvents. Solvents used for reactions or chromatography were either reagent grade or HPLC grade. Reactions were run under an argon atmosphere at ambient temperature unless otherwise noted. The following abbreviations are used, THF, tetrahydrofuran; DMF, *N,N*-dimethylformamide; DMSO, dimethyl sulfoxide; EDC, 1-[3-(dimethylamino)propyl]-3-ethylcarbodiimide hydrochloride.

Method A. 3-Aminopyrid-2-one (11). EtOH (300 mL) was added to a mixture of 10% (w/w) palladium on carbon catalyst (1 g) and 3-nitropyrid-2-one (**7**) (10 g, 71.43 mmol). The mixture was hydrogenated at atmospheric pressure and room temperature for 8 h. The catalyst was removed by filtration and washed with EtOH (2 \times 50 mL) and the EtOH evaporated to give the amine **11**⁴⁰ as a brown crystalline solid: 7.67 g (98%).

Method B. 3-[[(Benzyloxy)carbonyl]amino]pyrid-2-one (12). Benzyl chloroformate (13.085 g, 76.70 mmol) was added dropwise to a stirred suspension of Na₂CO₃ (16.26 g, 153.4 mmol) and 3-aminopyrid-2-one (**11**) (7.67 g, 69.73 mmol) in THF (20 mL). The mixture was stirred overnight, poured

into EtOAc (400 mL), washed with saturated aqueous NaHCO₃ (100 mL) and brine (100 mL), dried (Na₂SO₄), and evaporated. The resulting residue was purified by crystallization from MeOH to give **12** as a white crystalline solid: 10.7 g (63%); ¹H NMR δ 5.16 (2H, s), 6.21 (1H, t, *J* = 7 Hz), 7.08 (1H, d, *J* = 7 Hz), 7.30–7.44 (5H, m), 7.84 (1H, d, *J* = 7 Hz), 9.33 (1H, s), 11.95 (1H, br s); MS *m/z* 245 [M + 1]⁺.

Method C. 3-[[[(Benzyloxy)carbonyl]amino]-5-iodopyrid-2-one (13). To a stirred suspension of 3-[[[(benzyloxy)carbonyl]amino]pyrid-2-one (**12**) (8.0 g, 37.33 mmol) in dry CH₂Cl₂ (150 mL) was added *N*-iodosuccinimide (8.4 g, 37.33 mmol). The mixture was stirred (18 h), and the resulting precipitate was filtered to give the iodo compound **13** (3.1 g). The filtrate was concentrated to 30 mL and purified by chromatography using EtOAc:CH₂Cl₂ as the eluent (gradient, 0:100, 20:80, 25:75, 33:66, 50:50) to give additional iodo compound **13** (5.7 g): total yield, 8.8 g (46%); ¹H NMR δ 5.17 (2H, s), 7.33–7.45 (6H, m), 7.95 (1H, d, *J* = 7 Hz), 8.54 (1H, s), 12.14 (1H, s); MS *m/z* 371 [M + 1]⁺.

Method D. Ethyl [3-[[[(Benzyloxy)carbonyl]amino]-5-iodo-2-oxo-1,2-dihydro-1-pyridyl]acetate (16). A suspension of **13** (2.0 g, 5.405 mmol) in DMF (10 mL) was added to a suspension of NaH (0.156 g, 6.486 mmol) in DMF (10 mL) at 15–25 °C. After the mixture had stirred for 20 min, ethyl iodoacetate (1.453 g, 6.757 mmol) was added dropwise, maintaining the temperature below 20 °C. The mixture was stirred at room temperature for 3 h, poured into iced 1 N HCl (100 mL), and extracted with EtOAc (2 × 200 mL). The organic layers were washed with brine (2 × 100 mL), dried (Na₂SO₄), and evaporated to give a residue, which was purified by chromatography using EtOAc:CH₂Cl₂ as the eluent (gradient, 0:100, 3:97, 6:94) to give the ester **16**: 1.44 g (58%); ¹H NMR δ 1.21 (3H, t, *J* = 7 Hz), 4.14 (2H, q, *J* = 7 Hz), 4.72 (2H, s), 5.17 (2H, s), 7.32–7.44 (5H, m), 7.74 (1H, d, *J* = 2 Hz), 8.03 (1H, d, *J* = 2 Hz), 8.73 (1H, s); MS *m/z* 457 [M + 1]⁺.

Method E. Ethyl [3-[[[(Benzyloxy)carbonyl]amino]-5-(3-fluorobenzyl)-2-oxo-1,2-dihydro-1-pyridyl]acetate (17). To a suspension of freshly activated zinc dust (0.39 g, 6.039 mmol) in THF (5 mL) was added 3-fluorobenzyl bromide (0.76 g, 4.026 mmol) in THF (10 mL) at 20 °C. The solution was stirred for 3 h and dichloro[1,1'-bis(diphenylphosphino)ferrocene]palladium(II) (0.076 g, 0.100 mmol) was added followed by a solution of the iodide **16** (0.46 g, 1.007 mmol) in THF (10 mL), which was added dropwise. The mixture was stirred at room temperature for 5 h, at 50 °C for 4.5 h, and at room temperature for 18 h, poured into 1 N HCl (100 mL), and partitioned into EtOAc (3 × 100 mL). The combined organic extracts were dried (Na₂CO₃) and evaporated, and the resulting oil was purified by chromatography using EtOAc:CH₂Cl₂ (gradient, 0:100, 5:95, 10:90) as eluant to give **17**: 0.225 g (50%); ¹H NMR δ 1.20 (3H, t, *J* = 7 Hz), 4.14 (2H, q, *J* = 7 Hz), 3.73 (2H, s), 4.74 (2H, s), 5.13 (2H, s), 7.01–7.07 (3H, m), 7.31–7.41 (7H, m), 7.77 (1H, d, *J* = 2 Hz), 8.47 (1H, s); MS *m/z* 439 [M + 1]⁺.

Method F. 2-[3-[[[(Benzyloxy)carbonyl]amino]-5-(3-fluorobenzyl)-2-oxo-1,2-dihydro-1-pyridyl]-*N*-(3,3,3-trifluoro-2-hydroxy-1-isopropylpropyl)acetamide (6k). Aqueous 2 N NaOH (1.25 mL) was added to a solution of **17** (0.22 g, 0.501 mmol) in MeOH (8 mL). The mixture was stirred for 4 h and evaporated and the resulting residue triturated with 1 N HCl and extracted with EtOAc (3 × 25 mL). The combined organic extracts were dried (MgSO₄) and evaporated to yield [3-[[[(benzyloxy)carbonyl]amino]-5-(3-fluorobenzyl)-2-oxo-1,2-dihydro-1-pyridyl]acetic acid (0.21 g, 95%).

To the crude [3-[[[(benzyloxy)carbonyl]amino]-5-(3-fluorobenzyl)-2-oxo-1,2-dihydro-1-pyridyl]acetic acid (0.21 g, 0.478 mmol) in DMF (35 mL) was added 3-amino-4-methyl-1,1,1-trifluoro-2-pentanol hydrochloride (**21**) (0.117 g, 0.562 mmol), (dimethylamino)pyridine (0.140 g, 1.150 mmol), and EDC (0.113 g, 0.588 mmol). The mixture was stirred (18 h), added to 1 N HCl (100 mL), and extracted with EtOAc (2 × 100 mL). The combined organic extracts were washed with saturated aqueous NaHCO₃ (100 mL) and brine (100 mL), dried (Na₂SO₄), and evaporated to give a residue which was purified by chromatography, using EtOAc:CH₂Cl₂ (gradient, 0:100, 10:90, 20:80) as an eluent to give **6k**: 0.155 g (55%); ¹H NMR δ 0.87 (3H, d,

J = 7 Hz), 0.91 (3H, d, *J* = 7 Hz), 1.76–1.85 (1H, m), 3.72 (1H, s), 3.83 (1H, t, *J* = 9 Hz), 4.10–4.13 (1H, m), 4.49 (1H, d, *J* = 16 Hz), 4.75 (1H, d, *J* = 16 Hz), 5.12 (2H, s), 6.53 (1H, d, *J* = 7 Hz), 6.99–7.07 (3H, m), 7.23 (1H, d, *J* = 2 Hz), 7.29–7.38 (6H, m), 7.70 (1H, d, *J* = 2 Hz), 7.99 (1H, d, *J* = 10 Hz), 8.36 (1H, s); MS *m/z* 564 [M + 1]⁺.

Method G. 2-[3-[[[(Benzyloxy)carbonyl]amino]-5-(3-fluorobenzyl)-2-oxo-1,2-dihydro-1-pyridyl]-*N*-(3,3,3-trifluoro-1-isopropyl-2-oxopropyl)acetamide (5k). To a solution of EDC (0.51 g, 2.664 mmol) in DMSO (2 mL), toluene (4 mL), and dichloroacetic acid (0.14 g, 1.066 mmol) was added alcohol **6k** (0.15 g, 0.266 mmol). The mixture was stirred (18 h) and partitioned between EtOAc and saturated aqueous NaHCO₃. The organics were washed with brine (100 mL), dried (Na₂SO₄), evaporated, and purified by chromatography using CH₂Cl₂ as the eluent to give **5k** as a 1:1 mixture of the hydrate and nonhydrate forms: 0.120 g (80%); ¹H NMR δ 0.79–0.97 (6H, m), 2.21 (1H, m), 3.72 (2H, s), 4.06 (0.5H, m), 4.49–4.81 (2.5H, m), 5.13 (2H, s), 6.95–7.07 (3H, m), 7.22–7.40 (7H, m), 7.72 (1H, d, *J* = 2 Hz), 7.82 (0.5H, d, *J* = 11 Hz), 8.36 (1H, d, *J* = 11 Hz), 8.92 (0.5H, d, *J* = 6.5 Hz); MS *m/z* 562 [M + 1]⁺. Anal. (C₂₈H₂₇F₄O₅N₃·0.25H₂O) C, H, N.

Method H. 2-[3-[[[(Aminooxalyl)amino]-2-oxo-1,2-dihydro-1-pyridyl]-*N*-(3,3,3-trifluoro-1-isopropyl-2-oxopropyl)acetamide (5g). Compound **5e** (0.26 g, 0.665 mmol), the ammonium salt of 1-hydroxybenzotriazole (0.20 g, 1.220 mmol),⁴¹ and EDC (0.14 g, 0.731 mmol) in DMF (5 mL) were stirred (18 h). The mixture was partitioned between EtOAc (50 mL) and 1 N HCl (50 mL), and the organic layer was washed with saturated aqueous NaHCO₃ (50 mL), water (50 mL), and brine (50 mL), dried, evaporated, and purified by chromatography using EtOAc:CH₂Cl₂ (gradient, 1:1, 3:1) as the eluent to give **5g** as a white solid (mainly the unhydrated form): 80 mg (31%); mp 258–260 °C; ¹H NMR δ 0.94 (3H, d, *J* = 7 Hz), 0.96 (3H, d, *J* = 7 Hz), 2.2 (1H, m), 4.66 (1H, t, *J* = 6 Hz), 4.68–4.83 (2H, m), 6.35 (1H, t, *J* = 7 Hz), 7.43 (1H, dd, *J* = 2 and 7 Hz), 8.1 (1H, s), 8.26 (1H, dd, *J* = 2 and 7 Hz), 8.5 (1H, s), 8.9 (1H, d, *J* = 6 Hz), 9.9 (1H, s); MS *m/z* 391 [M + 1]⁺. Anal. (C₁₅H₁₇F₃N₄O₅·0.5H₂O) C, H, N.

Method I. 2-[3-[[[(Aminooxalyl)amino]-5-benzyl-2-oxo-1,2-dihydro-1-pyridyl]-*N*-(3,3,3-trifluoro-1-isopropyl-2-oxopropyl)acetamide (5w). Compound **5u** (0.35 g, 0.707 mmol) and concentrated ammonium hydroxide (1 mL) were combined in MeOH (1 mL) and allowed to stir for 3 h. The mixture was poured into EtOAc (50 mL), washed with 1 N HCl (50 mL), dried (Na₂SO₄), evaporated, and purified by chromatography using EtOAc:CH₂Cl₂ (gradient, 25:75, 50:50, 75:25) as the eluant to give **5w** as a white solid (as a 1:2 mixture of the hydrated and nonhydrated forms): 0.21 g (62%); mp 147–156 °C; ¹H NMR δ 0.8–1.0 (6H, m), 2.0–2.1 (0.33H, m), 2.1–2.2 (0.67H, m), 3.7 (2H, s), 4.1 (0.33H, m), 4.5–4.9 (2.67H, m), 7.1–7.5 (6H, m), 7.9–8.0 (0.33H, m), 8.12 (1H, s), 8.13 (1H, d, *J* = 2 Hz), 8.38 (1H, s), 8.9 (0.67H, d, *J* = 7 Hz), 9.9 (1H, d, *J* = 4 Hz); MS *m/z* 481 [M + 1]⁺. Anal. (C₂₂H₂₃F₃N₄O₅·0.5H₂O) C, H, N.

Method J. *N*-[2-[(*tert*-Butyldimethylsilyloxy]-3,3,3-trifluoro-1-isopropyl)-2-iodoacetamide (20). To solution of (2*RS*,3*SR*)-3-amino-1,1,1-trifluoro-4-methyl-2-pentanol hydrochloride (**21**) (20 g, 97 mmol) in THF (480 mL) was added 4-methylmorpholine (21.8 mL, 198 mmol) followed by slow addition of a solution of chloroacetyl chloride (7.7 mL, 97 mmol) in THF (40 mL). The solution was stirred (18 h), diluted with EtOAc (500 mL), and filtered to remove solids. The filtrate was washed with 1 M HCl, water, saturated aqueous NaHCO₃, and brine. The solution was dried and evaporated to give an oil.

To the crude oil in CH₂Cl₂ (96 mL) was added 2,6-lutidine (22.5 mL, 193 mmol) and *tert*-butyldimethylsilyl triflate (33 mL, 143 mmol). The mixture was stirred (12 h), diluted with EtOAc, and washed with 1 M HCl, saturated aqueous NaHCO₃, and brine. The organic solution was adsorbed onto silica gel (120 mL) by evaporation and purified by chromatography, eluting with EtOAc:hexane (gradient, 7:93 to 20:80), to give a white solid (20.5 g, 59%).

The white solid (15.5 g, 43 mmol) and NaI (19.3 g, 128 mmol) were stirred (18 h) in acetone (130 mL). The solution was

poured into water and the resulting precipitate filtered and washed with saturated aqueous sodium thiosulfate and water. The solid was purified by chromatography, eluting with EtOAc:hexane (gradient, 20:80–50:50), to give **20** (17.9 g, 92%) as a white solid: $^1\text{H NMR}$ δ 0.12 (3 H, s), 0.16 (3 H, s), 0.96 (15 H, m), 1.76 (1 H, m), 3.74 (2 H, s), 4.15 (1 H, q, $J = 6.6$ Hz), 6.51 (1H, d, $J = 10$ Hz); MS m/z 454 $[\text{M} + \text{H}]^+$.

Method K. 2-[3-[[**(Benzyloxy)carbonyl**]amino]-5-[4-(methoxycarbonyl)benzyl]-2-oxo-1,2-dihydro-1-pyridyl]-**N**-(3,3,3-trifluoro-2-hydroxy-1-isopropylpropyl)acetamide (**6t**). A 1 N solution of tetrabutylammonium fluoride (1.20 mL) in THF was added dropwise to a solution of **23** (0.749 g, 1.086 mmol) in THF (5 mL) with stirring. After 15 min, the reaction mixture was diluted with EtOAc (100 mL), washed with 1 N HCl (50 mL), saturated aqueous NaHCO_3 (50 mL), and brine (50 mL), dried, and evaporated. The resulting solid was purified by chromatography, eluting with EtOAc: CH_2Cl_2 (0:100, gradient, 5:90–50:50), to give the alcohol **6t**: 0.590 g (90%); $^1\text{H NMR}$ δ 0.88 (3H, d, $J = 7$ Hz), 0.91 (3H, d, $J = 7$ Hz), 1.7–2.0 (1H, m), 3.7 (2H, s), 3.8–3.9 (1H, m), 3.9 (3H, s), 4.1 (1H, m), 4.5 (1H, d, $J = 16$ Hz), 4.7 (1H, d, $J = 16$ Hz), 5.1 (2H, s), 6.5 (1H, d, $J = 7$ Hz), 7.2 (1H, d, $J = 2$ Hz), 7.3–7.4 (7H, m), 7.7 (1H, d, $J = 2$ Hz), 7.90 (2H, d, $J = 7$ Hz), 7.98 (1H, d, $J = 5$ Hz), 8.4 (1H, s); MS m/z 604 $[\text{M} + \text{H}]^+$.

Method L. 2-[3-[[**(Benzyloxy)carbonyl**]amino]-2-oxo-5-[4-(pivaloyloxy)benzyl]-1,2-dihydro-1-pyridyl]-**N**-(3,3,3-trifluoro-2-hydroxy-1-isopropylpropyl)acetamide (**6n**). Trifluoroacetic acid (3 mL) was added dropwise to **11** (0.320 g, 0.583 mmol) with stirring. After 30 min, the reaction mixture was diluted with CH_2Cl_2 (50 mL) and evaporated, diluted with chloroform (50 mL) and evaporated, diluted with diethyl ether (50 mL) and evaporated, and dried under high vacuum to give the crude acid intermediate. (2*RS*,3*SR*)-3-Amino-4-methyl-1,1,1-trifluoro-2-pentanol hydrochloride (0.149 g, 0.715 mmol), EDC (0.143 g, 0.748 mmol), and 4-(dimethylamino)pyridine (0.238 g, 1.951 mmol) were added to a solution of the crude acid (0.32 g) in DMF (30 mL) and stirred for 18 h. The mixture was added to 1 N HCl (100 mL), extracted with EtOAc (100 mL), washed with saturated aqueous NaHCO_3 (100 mL) and brine (100 mL), and evaporated to give a residue which was purified by chromatography, eluting with EtOAc: CH_2Cl_2 (0:100, 10:90), to give the alcohol **6n**: 0.220 g (57%); $^1\text{H NMR}$ δ 0.87 (3H, d, $J = 7$ Hz), 0.91 (3H, d, $J = 7$ Hz), 1.3 (9H, s), 1.7–1.9 (1H, m), 3.7 (2H, s), 3.8 (1H, m), 4.0–4.2 (1H, m), 4.5 (1H, d, $J = 16$ Hz), 4.7 (1H, d, $J = 16$ Hz), 5.1 (2H, s), 6.5 (1H, d, $J = 7$ Hz), 7.0 (2H, m), 7.2–7.4 (8H, m), 7.7 (1H, d, $J = 2$ Hz), 7.98 (1H, d, $J = 10$ Hz), 8.3 (1H, s); MS m/z 646 $[\text{M} + \text{H}]^+$.

Acknowledgment. We acknowledge Dr. Brian Masek for assistance with the molecular modeling, Drs. A. Shaw, C. A. Veale, P. D. Edwards, F. J. Brown, and D. J. Wolanin for helpful discussions, and Dr. J. C. Williams for evaluating selected compounds in the acute lung hemorrhagic model.

References

- Travis, J.; Dublin, A.; Potempa, J.; Watorek, W.; Kurdowska, A. Neutrophil Proteinases. *Ann. N. Y. Acad. Sci.* **1991**, *624*, 81–86.
- Janoff, A. Elastases and Emphysema. Current Assessment of the Protease-Antiprotease Hypothesis. *Am. Rev. Respir. Dis.* **1985**, *132*, 417–433.
- Eriksson, S. The Potential Role of Elastase Inhibitors in Emphysema Treatment. *Eur. Respir. J.* **1991**, *4*, 1041–1043.
- Snider, G. L.; Ciccolella, D. E.; Morris, S. M.; Stone, P. J.; Lucey, E. C. Putative Role of Neutrophil Elastase in the Pathogenesis of Emphysema. *Ann. N. Y. Acad. Sci.* **1991**, *624*, 45–59.
- Merritt, T. A.; Cochrane, C. G.; Holcomb, K.; Bohl, B.; Hallman, M.; Strayer, D.; Edwards, D.; Gluck, L. Elastase and α_1 -Proteinase Inhibitor Activity in Tracheal Aspirates During Respiratory Distress Syndrome. *J. Clin. Invest.* **1983**, *72*, 656–666.
- Petty, T. L. Protease Mechanisms in the Pathogenesis of Acute Lung Injury. *Ann. N. Y. Acad. Sci.* **1991**, *624*, 267–277.
- Nadel, J. A. Role of Mast Cell and Neutrophil Proteases in Airway Secretion. *Am. Rev. Respir. Dis.* **1991**, *144*, S48–S51.
- Jackson, A. H.; Hill, S. L.; Afford, S. C.; Stockley, R. A. Sputum Soluble Phase Proteins and Elastase Activity in Patients with Cystic Fibrosis. *J. Respir. Dis.* **1984**, *65*, 114–124.
- Nadel, J. A. Protease Actions on Airway Secretions. Relevance to Cystic Fibrosis. *Ann. N. Y. Acad. Sci.* **1991**, *624*, 286–296.
- Ekerot, L.; Ohlsson, K. Interactions of Granulocyte Proteases with Inhibitors in Rheumatoid Arthritis. *Adv. Exp. Med. Biol.* **1984**, *167*, 335–344.
- Turino, G. M. Natural History and Clinical Management of Emphysema in Patients with and without Alpha₁-Antitrypsin Inhibitor Deficiency. *Ann. N. Y. Acad. Sci.* **1991**, *624*, 18–29.
- Johnson, D.; Travis, J. Structural Evidence for Methionine at the Reactive Site of Human α_1 -Proteinase Inhibitor. *J. Biol. Chem.* **1978**, *253*, 7142–7144.
- Beatty, K.; Matteson, N.; Travis, J. Kinetic and Chemical Evidence for the Inability of Oxidised α_1 -Proteinase Inhibitor to Protect Lung Elastin from Elastolytic Degradation. *Hoppe-Segler's Z. Physiol. Chem.* **1984**, *365*, 731–736.
- Trainor, D. A. Synthetic inhibitors of human neutrophil elastase. *TIPS* **1987**, *8*, 303–307.
- Stein, R. L.; Strimpler, A. M.; Edwards, P. D.; Lewis, J. J.; Mauger, R. C.; Schwartz, J. A.; Stein, M. M.; Trainor, D. A.; Wildonger, R. A.; Zottola, M. A. Mechanism of Slow-Binding Inhibition of Human Leukocyte Elastase by Trifluoromethyl Ketones. *Biochemistry* **1987**, *26*, 2682–2689.
- Imperiali, B.; Abeles, R. H. Inhibition of Serine Proteases by Peptidyl Fluoromethyl Ketones. *Biochemistry* **1986**, *25*, 3260–3267.
- Peet, N. P.; Burkhart, J. P.; Angelastro, M. R.; Giroux, E. L.; Mehdi, S.; Bey, P.; Kolb, M.; Neises, B.; Schirlin, D. J. Synthesis of Peptidyl Fluoromethyl Ketones and Peptidyl α -Keto Esters as Inhibitors of Porcine Pancreatic Elastase, Human Neutrophil Elastase, and Rat and Human Neutrophil Cathepsin G. *J. Med. Chem.* **1990**, *33*, 394–407.
- Skiles, J. W.; Fuchs, V.; Miao, C.; Sorcek, R.; Grozinger, K. G.; Maudlin, S. C.; Vitous, J.; Mui, P. W.; Jacober, S.; Chow, G.; Matteo, M.; Skoog, M.; Weldon, S.; Possanza, G.; Keirns, J.; Letts, G.; Rosenthal, A. S. Inhibition of Human Leukocyte Elastase (HLE) by N-Substituted Peptidyl Trifluoromethyl Ketones. *J. Med. Chem.* **1992**, *35*, 641–662.
- Edwards, P. D.; Meyer, E. F., Jr.; Vijayalakshmi, J.; Tuthill, P. A.; Andisik, D. A.; Gomes, B.; Strimpler, A. Design, Synthesis, and Kinetic Evaluation of a Unique Class of Elastase Inhibitors, the Peptidyl α -ketobenzoxazoles, and the X-ray Crystal Structure of the Covalent Complex between Porcine Pancreatic Elastase and Ac-Ala-Pro-Val-2-Benzoxazole. *J. Am. Chem. Soc.* **1992**, *114*, 1854–1863.
- Doherty, J. B.; Ashe, B. M.; Argenbright, L. W.; Barker, P. L.; Bonney, R. J.; Chandler, G. O.; Dahlgren, M. E.; Dorn, C. P., Jr.; Finke, P. E.; Firestone, R. A.; Fletcher, D.; Hagemann, W. K.; Mumford, R.; O'Grady, L.; Maycock, A. L.; Pisano, J. M.; Shah, S. K.; Thompson, K. R.; Zimmermann, M. Cephalosporin Antibiotics Can Be Modified To Inhibit Human Leukocyte Elastase. *Nature* **1986**, *322*, 192–194.
- Williams, J. C.; Falcone, R. C.; Knee, C.; Stein, R. L.; Strimpler, A. M.; Reaves, B.; Giles, R. E.; Krell, R. D. Biologic Characterization of ICI 200,880 and ICI 200,355; Novel Inhibitors of Human Neutrophil Elastase. *Am. Rev. Respir. Dis.* **1991**, *144*, 875–883.
- Williams, J. C.; Stein, R. L.; Giles, R. E.; Krell, R. D. Biochemistry and Pharmacology of ICI 200,880, a Synthetic Peptide Inhibitor of Human Neutrophil Elastase. *Ann. N. Y. Acad. Sci.* **1991**, *624*, 230–243.
- Takahashi, L. H.; Radhakrishnan, R.; Rosenfield, R. E., Jr.; Meyer, E. F., Jr.; Trainor, D. A.; Stein, M. X-Ray Diffraction Analysis of the Inhibition of Porcine Pancreatic Elastase by a Peptidyl Trifluoromethylketone. *J. Mol. Biol.* **1988**, *201*, 423–428.
- Fearon, K.; Spaltenstein, A.; Hopkins, P. B.; Gelb, M. H. Fluoro Ketone Containing Peptides as Inhibitors of Human Renin. *J. Med. Chem.* **1987**, *30*, 1617–1622.
- Pfitzner, K. E.; Moffatt, J. G. Sulfoxide-Carboodiimide Reactions. I. A Facile Oxidation of Alcohols. *J. Am. Chem. Soc.* **1965**, *87*, 5661–5670.
- P. D. Edwards, personal communication.
- Hayashi, T.; Konishi, M.; Kobori, Y.; Kumada, M.; Higuchi, T.; Hirotsu, K. Dichloro[1,1'-bis(diphenylphosphino)ferrocene]palladium (II): An Effective Catalyst for Cross-Coupling of Secondary and Primary Alkyl Grignard and Alkylzinc Reagents with Organic Halides. *J. Am. Chem. Soc.* **1984**, *106*, 158–163.
- Bode, W.; Meyer, E., Jr.; Powers, J. C. Human Leukocyte and Porcine Pancreatic Elastase: X-Ray Crystal Structures, Mechanism, Substrate Specificity, and Mechanism-Based Inhibitors. *Biochemistry* **1989**, *28*, 1951–1963 and references therein.
- Bode, W.; Wei, A.-Z.; Huber, R.; Meyer, E.; Travis, J.; Neumann, S. X-ray crystal structure of the complex of human leukocyte elastase (PMN elastase) and the third domain of the turkey ovomucoid inhibitor. *EMBO J.* **1986**, *5*, 2453–2458.

- (30) QUANTA was used to select the desired residues. These included His 40-Cys 42, His 57-Asn 61, Leu 99-Asp 102, Leu 143, Ile 151-Ala 152, Arg 177, Val 190-Ser 195, and Ala 213-Cys 220. The C-termini of all fragments were capped as the N-methyl amides and the N-termini as the acetamide. The positions of the capping fragments mimic that of the preceding or succeeding residues. The model was then transferred to ENIGMA³⁰ where bond multiplicities were corrected and hydrogens added.
- (31) ENIGMA is an in-house molecular graphics program, ZENECA Inc., Wilmington, DE 19897.
- (32) AESOP is an in-house molecular mechanics program, ZENECA Inc., Wilmington, DE 19897, derived in part from BIGSTRN-3 (QCPE 514): Nachbar, R.; Mislow, K. *QCPE Bull.* **1986**, *6*, 96. AESOP employs MM2 force field parameters, see: Allinger, N. L. *QCPE Bull.* **1980**, *12*, 395.
- (33) It was necessary to add extra residues to the model to avoid unrealistically distorting the active site model. The added residues were Ser 54-Ala 56, Gly 189, Gly 196-Ser 197, and Asp 226-Ala 229 all capped appropriately as described above. The amide linkage between Ile 16 and Val 17 was also included as a methylacetamide fragment. The parts of the model allowed to optimize were the His 57 side chain, the inhibitor, Phe 192-Ser 195, the Cys 191 backbone, the Val 190 carbonyl, the Val 216 side chain and NH, Ala 213 (except the NH), the Ser 214 backbone, and the Phe 215 backbone and α -carbon.
- (34) Wei, A.-Z.; Mayr, I.; Bode, W. The refined 2.3 Å crystal structure of human leukocyte elastase in a complex with a valine chloromethyl ketone inhibitor. *FEBS Lett.* **1988**, *234*, 367-373.
- (35) D. J. Wolanin, personal communication.
- (36) Skiles, J. W.; Miao, C.; Sorcek, R.; Maudlin, S. C.; Mui, P. W.; Jacober, S.; Chow, G.; Skoog, M.; Weldon, S.; Possanza, G.; Keirns, J.; Letts, G.; Rosenthal, A. S. Inhibition of Human Leukocyte Elastase by N-Substituted Peptides containing α,α -Difluorostatone Residues at P1. *J. Med. Chem.* **1992**, *35*, 4795-4808.
- (37) A recent paper has described the incorporation of lactams into TFMK peptides as P3-P2 dipeptide replacements. Skiles, J. W.; Sorcek, R.; Jacober, S.; Miao, C.; Mui, P. W.; McNeil, D.; Rosenthal, A. S. Elastase inhibitors containing conformationally restricted lactams as P3-P2 dipeptide replacements. *Bioorg. Med. Chem. Lett.* **1993**, *3*, 773-778.
- (38) Bergeson, S. H.; Edwards, P. D.; Krell, R. D.; Shaw, A.; Stein, M. M.; Strimpler, A. M.; Trainor, D. A.; Wildonger, R. A.; Wolanin, D. J. Inhibition of Human Leukocyte Elastase By Peptide Trifluoromethyl Ketones. *Abstracts of Papers*, 193rd National Meeting of the American Chemical Society, Denver, CO, April 5-10, 1987; American Chemical Society: Washington, DC, 1987; MEDI 0001.
- (39) Brown, F. J.; Andisik, D. W.; Bernstein, P. R.; Bryant, C. B.; Ceccarelli, C.; Damewood, J. R.; Edwards, P. D.; Earley, R. A.; Feeney, S.; Green, R. C.; Gomes, B.; Kosmider, B. J.; Krell, R. D.; Shaw, A.; Steelman, G. B.; Thomas, R. M.; Vacek, E. P.; Veale, C. A.; Tuthill, P. A.; Warner, P.; Williams, J. C.; Wolanin, D. J.; Woolson, S. A. Design of Orally Active, Non-peptidic Inhibitors of Human Leukocyte Elastase. *J. Med. Chem.* **1994**, *37*, 1259-1261.
- (40) Oklobdzija, M.; Comisso, G.; Decorte, E.; Fajdiga, T.; Gratton, G.; Moimas, F.; Toso, R.; Sunjic, V. Novel Synthesis of 5,11-dihydro-6H-pyrido[2,3-b][1,4]benzodiazepin-6-ones and related studies. Part I. *J. Heterocycl. Chem.* **1983**, *20*, 1329-1334.
- (41) Bajusz, S.; Ronai, A. Z.; Szekely, J. I.; Graf, L.; Dunai-Kovacs, Z.; Berzetei, I. A Superactive Antinociceptive Pentapeptide, (D-Met², Pro⁵)-Enkephalinamide. *FEBS Lett.* **1977**, *76*, 91.